Chapter 4

Stearate intercalated layered double hydroxides: effect on the physical properties of dextrin-alginate films

Expanded version of article submitted to *Journal of Materials Science*.

Abstract

The effect of stearate intercalated layered double hydroxides (LDH-SA) on the water vapour permeability (WVP) and mechanical properties of glycerol plasticized dextrin-alginate films were tested. The LDH $Mg_4Al_2(OH)_{12}CO_3{\cdot}3H_2O$ and stearic acid (SA) were reacted in different mass ratios within the film solutions. The filler (SA and LDH) concentration was fixed at 16% m/m of the dried films. Infrared spectroscopy verified that the SA did indeed intercalate. WVP measurements showed a broad range of minima around filler compositions of 50-80% SA (and 50-20% LDH). The Young's moduli of the films showed a maximum increase of 213% around the filler composition of 60% SA (40% LDH). From the interlayer distances and intensities of the basal reflections of the LDH-SA (as determined from X-ray diffraction, XRD) and the increased Young's moduli it was concluded that delamination and exfoliation of the LDH-SA took place. A layered and oriented microscopic structure was seen by scanning electron microscopy (SEM).

Keywords: Layered double hydroxides, stearic acid, intercalation, starch, dextrin, alginate, edible films, water vapour permeability, Young's modulus, exfoliation, delamination, cross-linking

4.1. Introduction

Edible films are used to protect foodstuff from water vapour and oxygen in their environment and to prevent water moving from one part to another in multi-component foodstuffs, for example to separate the filling or sauce from the dough of pizzas or pies. Most edible film-forming polymers or hydrocolloids (such as starch, sodium alginate, and sodium caseinate) are hydrophilic and pose no barrier against water vapour, and becomes soggy in contact with water. Lipid films are good barriers against water, but have little structural integrity. This problem has been overcome using laminates of hydrocolloid and wax films and also by making emulsions of the wax or lipid within the hydrocolloid solution. Waxes such as beeswax and stearic acid are emulsified within the surface-active sodium alginate or sodium caseinate and their blends with starch. [1,2,3]

Polymer-layered clay nanocomposites are filled polymers in which at least one of the dimensions of the filler is in the nanometre range (less than 100 nm). Nanocomposites in general have increased modulus, strength and heat resistance, as well as decreased gas permeability and flammability in comparison to the pristine polymer. [4] Studies were done on preparing composites of starch with kaolin [5], Ca^{2+} hectorite [6] and kaolinite, hectorite, layered double hydroxide (LDH) and brucite [7]. These studies focused mainly on the mechanical properties and microstructure of the composites as well as determining whether exfoliation took place by means of X-ray diffraction. These platelet fillers, however, can ideally be used to reduce the WVP of hydrophilic polymers such as starch or alginate.

The water vapour permeability (WVP) and also the permeability to large organic molecules (or pharmaceuticals) of sodium alginate and sodium caseinate films can be reduced by cross-linking with polyvalent cations, e.g. Ca^{2+}. This can be done by immersing films in solutions of Ca^{2+} salts [3] or by *in situ* leaching Ca^{2+} ions from insoluble $CaCO_3$ by acids [8]. This mechanism might play a role in the

current system that is composed of an insoluble layered double hydroxide and stearic acid.

Hydrotalcite is an anionic clay mineral with the composition $Mg_6Al_2(OH)_{16}CO_3.4H_2O$. It has the same layered structure as brucite [$Mg(OH)_2$] but with some of the Mg^{2+} ions substituted by Al^{3+} ions. The presence of the Al^{3+} ions gives rise to a residual positive charge in the layers. This positive charge is balanced by anions such as CO_3^{2-}, Cl^- and NO_3^- or organic anions in the interlayer. [9] A range of compositions is possible in terms of bivalent and trivalent cations and of their relative amounts. These types of compounds are more generally referred to as layered double hydroxides (LDHs).

In the present study a combination of an LDH [$Mg_4Al_2(OH)_{12}CO_3{\cdot}3H_2O$] and stearic acid (SA) was used to reduce the WVP of glycerol-plasticized dextrin-alginate films. Ideally the SA would intercalate into the LDH structure to form LDH-SA during the film solution preparation. Stearate and other surfactant intercalated LDHs have large, plate-like microscopic structures [10,11] and this extended plate-like structures would lower the WVP of the dextrin-alginate films depending on their relative orientation within the films.

4.2. Experimental

4.2.1. Materials

The materials used, their source of origin, and their respective roles are given in Table 4-1.

Table 4-1 Components of the films and their roles.

Component name	From	Role
Dextrin, Stydex 074030	African Products (Pty.) Ltd, South Africa.	Biodegradable polymer
Sodium Alginate (E401), Manugel GMB, viscosity of 1% solution is 185 cps.	Kelco International Limited	Biodegradable polymer, film former, emulsion stabilizer (due to high viscosity), prevent agglomeration of LDH-SA
99% Glycerol	Merck, UNILAB®	Plasticizer
85% Stearic acid	Merck	Hydrophobic, intercalate into LDH.
LDH, $Mg_4Al_2(OH)_{12}CO_3{\cdot}3H_2O$ Particle size distribution by Mastersizer 2000 (Malvern Instruments): d(0,1): 0,694 μm; d(0,5): 5,062 μm and d(0,9): 23,925 μm. The XRF analysis is given in Appendix B.	Chamotte Holdings (Pty.) Ltd., South Africa	Filler, intercalated by SA.
Talc	Sigma-Aldrich, < 10 micron, $3MgO.4SiO_2.H_2O$	Filler, cannot be intercalated by SA. Coated and dispersed by SA.
Bentonite Ocean Clear	Boland Base Minerals, South Africa	Filler, cannot be intercalated by SA, coated and dispersed by SA.
Foamaster 8034	Cognis	Prevent foam formation due to CO_2 release.
Deionised water or tap water		Solvent
Ethanol, rectified 96%	Dana Chemicals	Solvent

4.2.2. Film production procedure

Wu *et al*. [1] attempted to lower the WVP of starch-alginate films by using, amongst others, SA. Their recipe was followed (Table 4-2) except that lecithin (emulsifier) was not used. The LDH, $Mg_4Al_2(OH)_{12}CO_3{\cdot}3H_2O$, was used additionally to the recipe of Wu *et al.* [1]. The ratio of SA and LDH was varied to determine its effect on WVP and Young's modulus. The SA and LDH together are referred to as the filler, which can consist of 100% SA, 100% LDH or any ratio in between. This filler content was kept constant at 16.56% m/m of the dried film, which is similar to the amount used by Wu *et al.* [1]. Films are referred to in terms of the SA content of the filler in the Figures and by annotations such as 60SA/40LDH for a film where the filler consists of 60% SA and 40% LDH by mass. CO_2 is released during the intercalation of stearate into LDH and this necessitated the use of a defoamer.

Table 4-2 Relative amounts of the different components in the films solutions and dry films.

Constituent	Typical amounts / g	% in film solution	% in dried film
Dextrin	2,5	2,78	41,39
Sodium alginate	1	1,11	16,56
Glycerol	1,4	1,55	23,18
SA	0 - 1	0 - 1,11	0 - 16,56
LDH	1 - 0	1,11 - 0	16,56 - 0
Defoamer	0,14	0,16	2,32
Water	60	66,64	-
Ethanol	24	26,65	-

Dextrin, sodium alginate and the LDH were mixed and crushed in a mortar and pestle. This procedure broke the LDH particles down by shear forces. The presence of the LDH also prevented the alginate from forming lumps during dissolution. The powdered mixture was slowly added to the water, ethanol, glycerol and SA solution at 78°C. A reaction time of one hour was used

throughout. Although the defoamer was effective, the mixtures were ultrasonicated in warm water to ensure release of all trapped bubbles still present. 8 g portions of the solutions were cast into metal rings of approximately 67 mm diameter (Fig. 4-1) to prepare samples for WVP analyses. 45 g portions were cast into 150 mm square metal holders that were placed on a non-stick silicone sheet (Silicone zone®). The samples were left to dry at room temperature and then removed by peeling. The films were cut into 45 mm diameter circles for WVP tests or punched into dumbbell shapes (6 mm wide, 35 mm gauge length, 115 mm total length) for tensile testing. Samples were conditioned for two weeks at 23 ± 2 °C, 75 % RH (saturated NaCl solution [12]) prior to analysis.

One film was made with tap water to determine whether the Ca^{2+} ions would have a negative effect (by reducing the alginate solubility) or a positive effect (by cross-linking the alginate) on the WVP.

Figure 4-1 Casting of film solution into metal rings.

4.2.3. Characterization

4.2.3.1. *Fourier Transform Infrared spectroscopy (FTIR)*

A Perkin Elmer Spectrum RX I FT-IR System was used to scan the infrared transmittance through a KBr (Uvasol, potassium bromide, Merck) pellet 32 times at a resolution of 2 cm^{-1}. The averaged spectrum was background-corrected using a pure KBr pellet run under similar conditions. The pellets were prepared with approximately 2 mg of sample and 100 mg of KBr. The 2 mg powder samples were obtained by diluting the film solution with excess deionised water in order to release the insoluble LDH-SA. It was subsequently recovered by centrifugation, dried and ground. This was done in order to enable the observation of carboxylate vibrations of the intercalated stearate, which is otherwise overshadowed by the carboxylate peaks of the sodium alginate.

4.2.3.2. *X-ray Diffraction (XRD)*

The XRD analyses were done on a Siemens D500 X-ray system equipped with a 2.2 kW Cu long fine focus tube, variable slit and secondary graphite monochromator. The system is computer controlled using SIEMENS DIFFRAC ^{Plus} software. The goniometer was set to reflection mode. The films were placed on a no-background silicon (Si) wafer before placing it onto the aluminium sample holder to prevent aluminium peaks from being seen. Samples were scanned from 1 to 40° 2θ with Cu K_α radiation (1.5418 Å) at a speed of 0.02° 2θ, with a recording time of 2 s per step and generator settings of 40 kV and 30 mA.

4.2.3.3. *Scanning Electron Microscopy (SEM)*

The film samples were freeze fractured by dipping into liquid nitrogen and then breaking the brittle film. The broken cross-sections of the films were studied. These were coated with chromium in a high resolution ion beam coater, Gatan model 681 (Warrendale, PA, USA) to prevent charge build-up due to its low conductivity. Samples were then studied with the JSM-6000F field emission scanning electron microscope (JEOL, Tokyo, Japan).

4.2.3.4. Optical microscopy

A drop of the film solution was placed between two microscope slides and studied under 40 times magnification with a Leica DME optical microscope with built-in digital camera.

4.2.3.5. *Water Vapour Permeability (WVP)*

The cast and dried films were cut into discs of appropriate size for the WVP cups. A Mitutoyo Digimatic Indicator was used to determine the thickness of each disc at 9 positions. The measured thicknesses varied between 130 and 140 μm. Additional films were prepared in order to determine the effect of thickness on WVP of films of differing compositions. In all cases at least four discs per formulation were tested. Film discs were mounted on cups filled with dried silica gel (Fig. 4-2) and placed in a desiccator filled with saturated NaCl solution in contact with excess NaCl to obtain 75% relative humidity (RH) at 23 ± 2 °C [12]. Films derived from emulsions always have a shiny side (bottom) and a dull side due to accumulation of lower density wax (or fatty acid) at the top. Therefore, the measured WVP depended on which side faced which relative humidity. [3] Care was taken to always place the shiny (more hydrophilic) side facing the 0% RH side.

A WVP test of the best performing film was carried out at 38 °C/90 %RH in order to determine its performance (good, moderate or poor) according to the classification scheme of Krochta *et al.* [13]

Figure 4-2 Water vapour permeability test setup.

4.2.3.6. *Tensile properties*

Films were allowed to condition for at least two weeks before testing, so that results would be comparable in terms of the age of the samples. The thickness of the samples were tested at three positions within the middle portion of the dumbbells and averaged. The measured thicknesses ranged from 110 to 130 μm. Samples were tested at a strain rate of 1 mm/min on a LRX Plus instrument from Lloyd Instruments, and results were analysed using Nexygen software. The software calculated the Young's moduli. Tests were performed at 25 °C at ambient humidity (30-50% RH). Three samples of each formulation were tested and averaged.

4.3. Results and Discussion

4.3.1. Fourier Transform Infrared spectroscopy (FTIR)

The FTIR spectrum of the LDH-SA intercalates obtained from the 60SA/40LDH film (Fig. 4-3) revealed that all the stearic acid reacted because the ν(C=O) stretching vibration at 1702 cm^{-1} was absent. The carboxylate (COO-)

asymmetric stretching vibrations were at 1539 cm^{-1}, 1554 cm^{-1} and 1576 cm^{-1}, which correlates well with the carboxylate asymmetric stretching vibrations (1542 cm^{-1}, 1557 cm^{-1} and 1589 cm^{-1}) obtained by Borja *et al.* [14] for meristate intercalated Mg_3Al-LDH. The weak peak at 1725 cm^{-1} was also seen by Borja *et al.* [14] at 1720 cm^{-1} and can be attributed to the intercalation of the acid (COOH). Therefore, the same intercalation product was obtained in these aqueous film solutions as was obtained by the ion exchange of the Cl^- ion in LDH-Cl by fatty acids in ethanol [14], and not the Mg/Al salt of the fatty acid. The presence of a peak at 1366 cm^{-1}, attested to the fact that all the carbonate counter-ions did not react. Some unreacted carbonate remained no matter how large an amount of SA was used to react with the carbonate species.

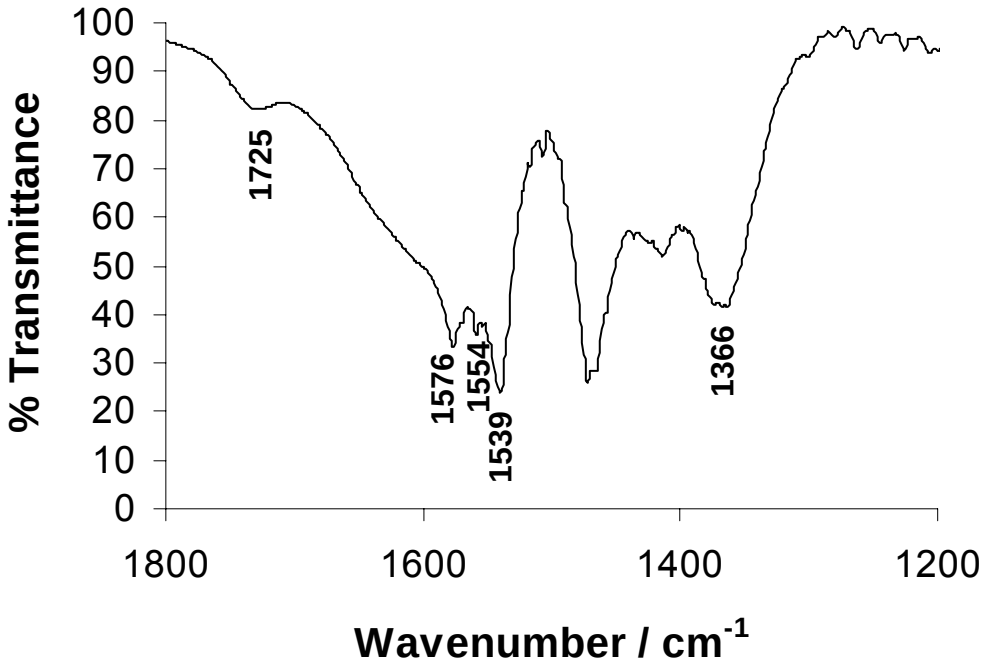

Figure 4-3 FTIR spectrum of the LDH-SA intercalates isolated from the 60SA/40LDH film solution, indicating complete ionisation and intercalation of SA together with some carbonate anions (1366 cm^{-1}).

4.3.2. Water Vapour Permeability (WVP)

The water permeability of hydrophilic films depends on the films moisture content. In the WVP experiment the film separates a region of high humidity from one of low humidity. Therefore there is also a gradient in the moisture content across the film. Owing to concentration polarization, this gradient depends on the film thickness. The consequence is that, unlike hydrophobic polymer films, the WVP of hydrophilic films depends on film thickness. This was previously noted by McHugh *et al.* [15].

Fig. 4-4 shows the WVP of several films. The WVP of blank films (only dextrin, alginate and glycerol, no LDH or SA) as well as the films with only SA or only LDH were thickness dependent and the values fell on the same straight line (WVP = 0.187x + 1.01, R^2 = 0.9928, Fig. 4-4). The WVP of films with a combination of LDH and SA, however, was independent of the thickness. Therefore, the combination of LDH and SA was more successful in producing films with hydrophobic characteristics (water vapour barrier properties) than SA alone. The raw data and calculations relating to Figure 4-4 can be seen in Table A-4 and A-5 in Appendix D. The method for calculating the WVP is also described in Appendix D.

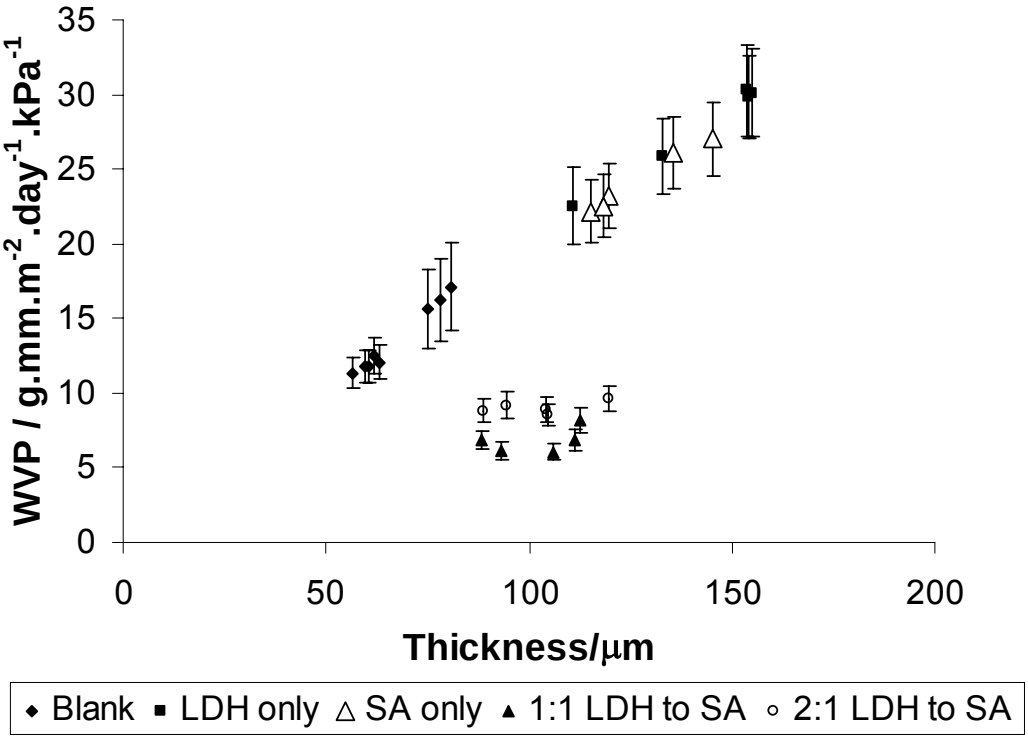

Figure 4-4 Thickness dependence of WVP of films with no filler, SA only or LDH only showing hydrophilic tendencies and those with combinations of SA and LDH showing hydrophobic tendencies.

For the films with constant thickness and amount of filler, a broad minimum in the WVP is observed at filler compositions ranging from 80SA/20LDH to 50SA/50LDH (Fig. 4-5). These results were explained and corroborated by SEM, XRD and tensile (Young's modulus) data. The raw data and calculations relating to Figure 4-5 can be seen in Table A-6 and A-7 in Appendix D.

The film with 100% SA in the filler, showed only a 17% decrease in the WVP. This is in good agreement with the results obtained by Wu *et al*. [1] for meat patties wrapped in starch/alginate/glycerol/SA films in relation to starch/alginate/glycerol films. The replacement of only 20% of the SA by the LDH, however, caused the WVP to decrease to 80% of that of the blank film (Fig. 4-5).

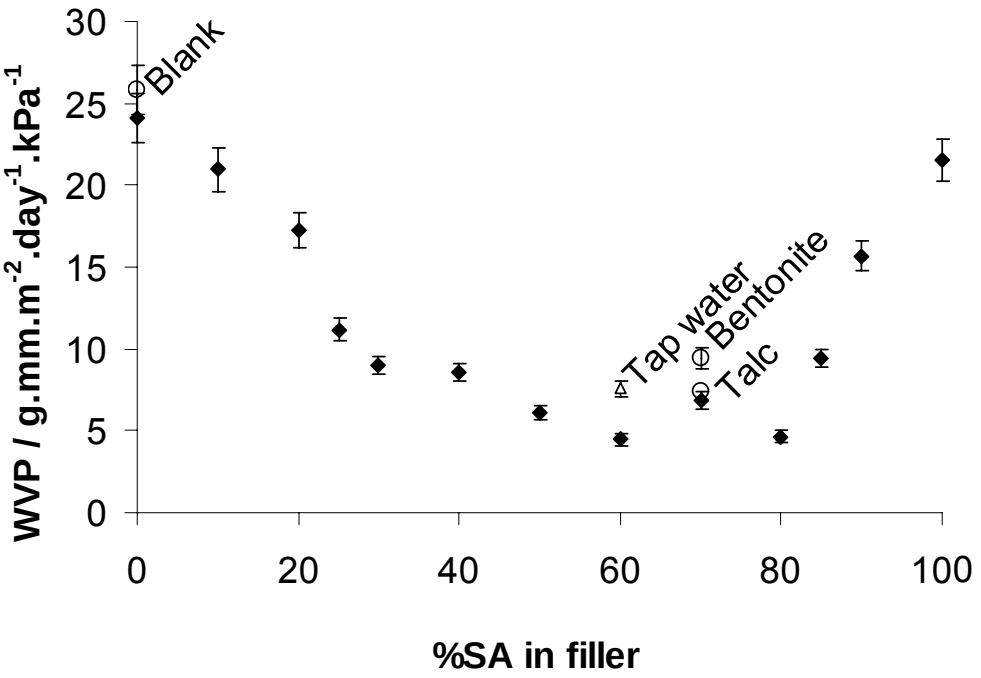

Figure 4-5 WVP measurements of constant-thickness films with fillers varying from 100SA/0LDH to 0SA/100LDH, showing a wide range of filler compositions yielding a minimum in the WVP.

When using tap water, one would expect the Ca^{2+} and Mg^{2+} ions to bind to the alginate, cross-linking it and thus improving the WVP, but the Ca^{2+} ions would decrease the solubility of the alginate which could, in turn, be detrimental to film formation. The use of tap water, however, had no detrimental effects on the results, as the WVP value fell within the variation in WVP seen within the curve (Fig. 4-5). This is beneficial since the water does not have to be demineralised or deionised for large-scale applications.

Films containing other sheet-like fillers at the same mass % dosage level, i.e. talc and bentonite showed a similar WVP (Fig. 4-5). Therefore, the WVP reached a minimum due to the improved dispersion of the LDH, talc and bentonite into the polymer matrices by the SA, a conclusion which is also corroborated by SEM results.

The 60SA/40LDH film which was also tested at 38°C and 90% RH, had a WVP of 13.5 ± 0.5 g.mm.m^{-2}.day^{-1}.kPa^{-1}, which is close to the border between the poor (10-100 g.mm.m^{-2}.day^{-1}.kPa^{-1}) and moderate (0.1-10 g.mm.m^{-2}.day^{-1}.kPa^{-1}) WVP regions according to the categorization of Krochta *et al*. [13]. In order to produce edible films or paper coatings with better performance in terms of WVP, the dextrin, which has poor WVP characteristics, could be replaced by polymers such as methyl cellulose, hydroxypropyl methyl cellulose, corn zein (protein), wheat gluten, poly(lactic acid) or cellulose acetate, which reside in the moderate WVP category according to Krochta *et al.* [13] Sodium alginate could also be replaced by sodium carboxymethyl cellulose in order to increase the hydrophobicity of the films.

4.3.3. Scanning Electron Microscopy (SEM)

The microstructures of the films with filler compositions of 100SA/0LDH through to 0SA/100LDH are shown in Figs. 4-6 (A-L). The SA could not alter the WVP characteristics of the matrix because the SA did not intimately mix with it, but formed dispersed globules (Fig. 4-6B) rather than oriented high aspect ratio sheets. The decrease in WVP (Fig. 4-5) corresponded to the presence of flat (white) plate-like structures (200-1000 nm thick and > 20 μm long) in the microstructure. The LDH-SA intercalates agglomerated in starch or dextrin solutions alone, but the viscous surface-active sodium alginate helped to disperse it into the dextrin-alginate solutions. These structures were first seen at filler composition 80SA/20LDH (Fig. 4-6D), where the reduction in WVP occurs. Beyond the filler composition of 50SA/50LDH (Fig. 4-6G), these structures gradually disappeared and the WVP increased again to higher values. These flat structures are typical of the surfactant intercalated LDHs. [10,11] Long crevices can also be seen where the LDH-SA were pulled out of the matrix due to poor adhesion. Using, for example, 12-hydroxy stearic acid instead of SA could improve the adhesion and compatibility of the intercalated clays with the hydrophilic matrix. The more hydrophobic polymers mentioned previously could

also improve adhesion to the LDH-SA intercalates, reducing pullout and increasing Young's modulus.

The films with bentonite and talc (Figs. 4-6M and 4-6N) also had an oriented structure due to the orientation of the filler particles. Wilhelm *et al*. [6] also observed the orientation of hectorite within fractured starch films. This orientation and dispersion of the fillers, therefore, account for the similar WVP results obtained for films with the same mass % LDH, talc or bentonite and SA.

LDH particles usually have sand-rose structures (Fig. 4-6O). The particles consist of many intergrown smaller particles that reduce accessibility to the surface area as a whole. [11] In Fig. 4-6P a fully intact LDH particulate is shown, which was released from the sand-rose structure and was captured and oriented within the larger plate-like structure of the LDH-SA. Under the influence of the SA the crystallites were aligned and reacted to form the LDH-SA layered structure (thickness ca. 100 nm, Fig. 4-6Q), with increased accessibility to the surfaces of the particles. If completely intercalated, the 100 nm thick plates could be interpreted as 20 layers of the LDH-SA (*ca.* 50 Å interlayer distances according to XRD). If intercalation did not take place, the 100 nm implies 131 layers (7.6 Å interlayer distances). Clearly, exfoliation to single layers did not occur. Single layer exfoliation would not be observable by SEM. According to He *et al.* [16] LDH crystals are only stable when they form stacking structures of approximately 20 layers. According to XRD two phases were present, namely LDH-SA and unreacted LDH-CO_3. Therefore, the plate-like structures probably consist of between 20 and 131 layers.

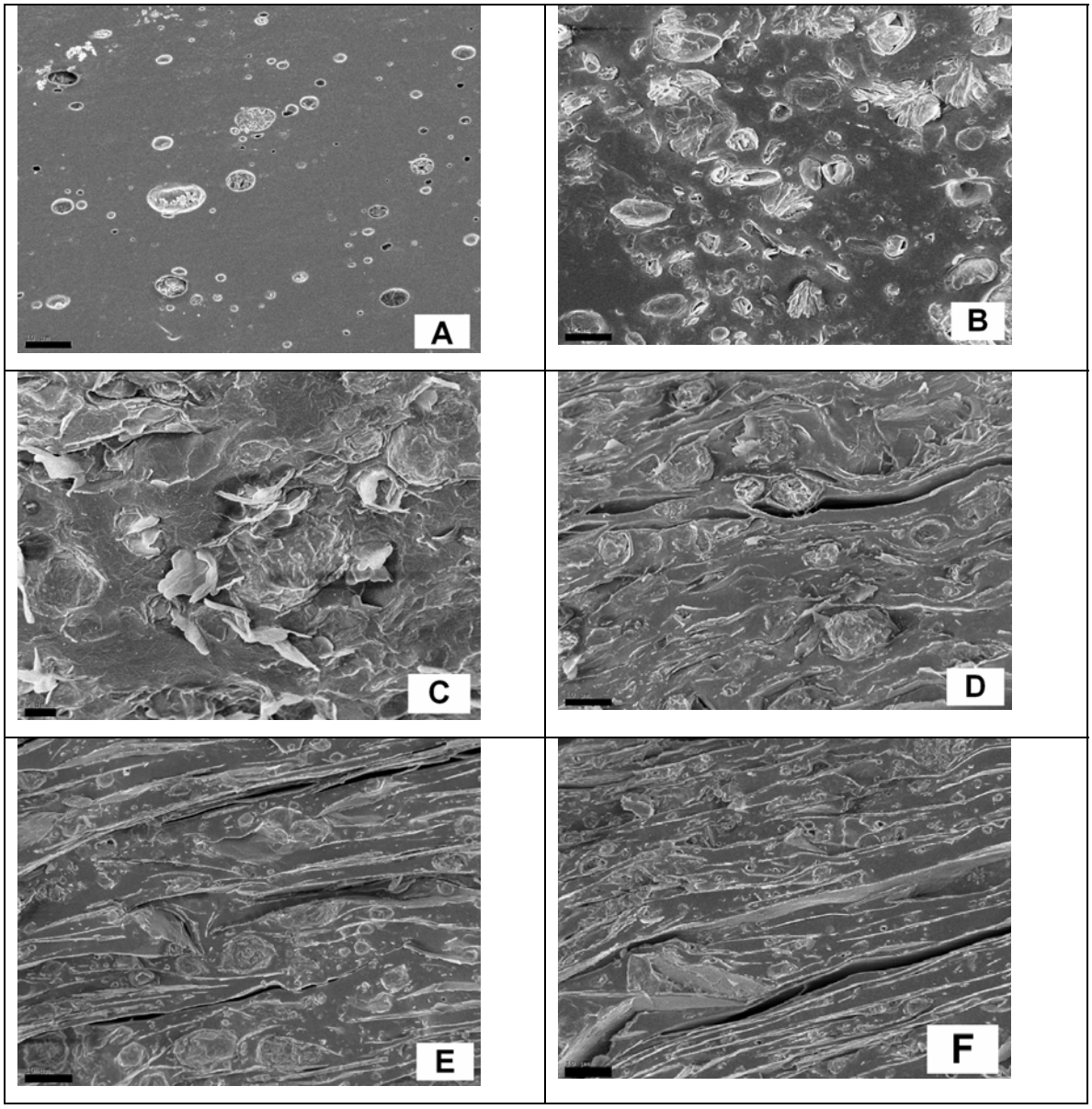

Figure 4-6 Scanning electron micrographs of the films.

A) Blank film. Undissolved alginic acid particles can be seen. Bar is 10 μm.

B) 100SA/0LDH. Some emulsified pockets of stearic acid can be seen. Bar is 10 μm.

C) 90SA/10LDH. Small, unoriented flat products of the SA-LDH reaction can be seen. Bar is 5 μm.

D) 80SA/20LDH. The reaction product of the SA and LDH were larger and more oriented. Bar is 10 μm.

E) 70SA/30LDH. The LDH-SA intercalate formed long, flat structures. Bar is 10 μm.

F) 60SA/40LDH. The LDH-SA intercalate formed long, flat structures. Bar is 10 μm.

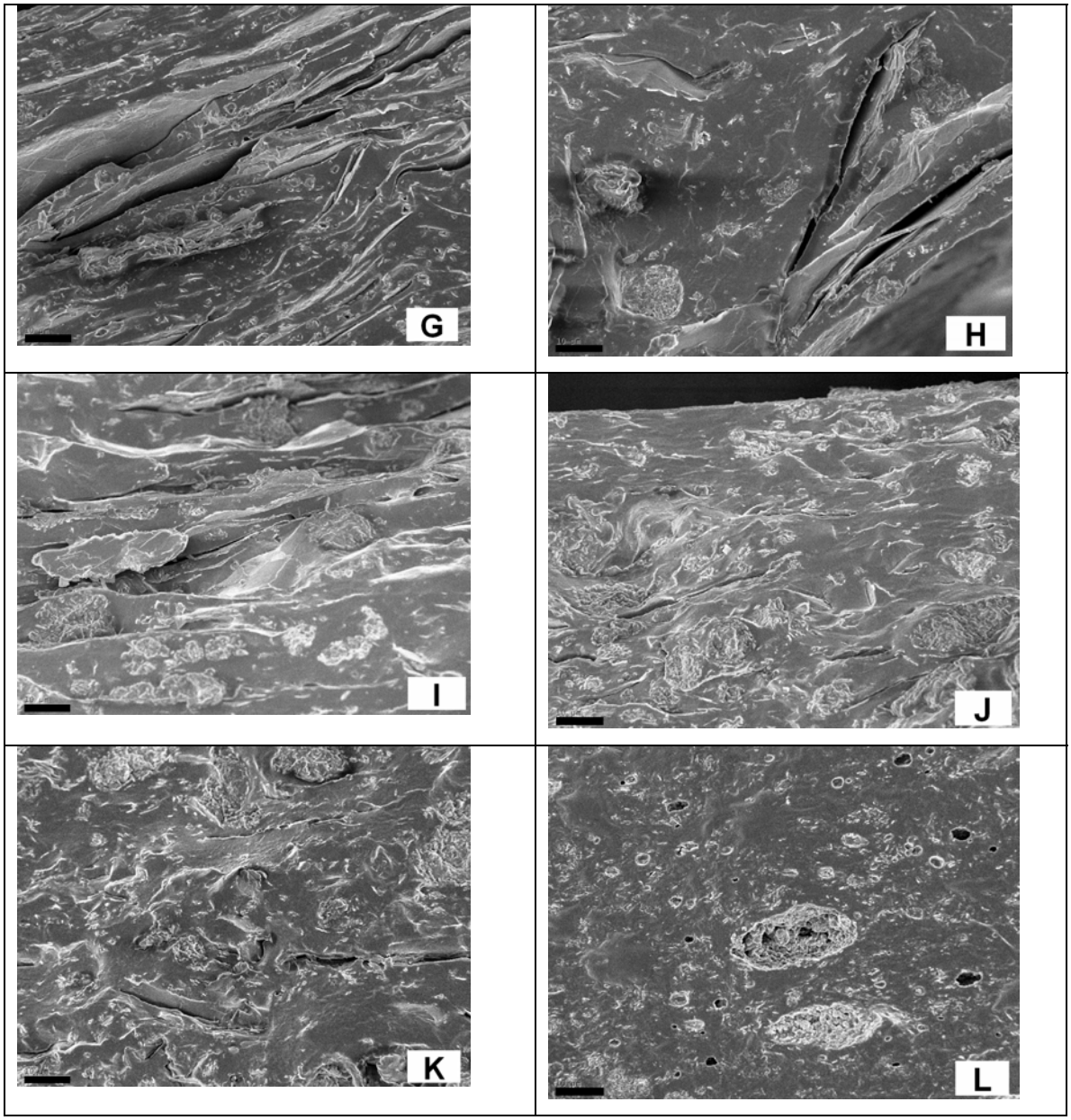

Figure 4-6 Scanning electron micrographs of the films.

G) 50SA/50LDH. The LDH-SA was smaller and less oriented. Bar is 10 μm.

H) 40SA/60LDH. Bar is 10 μm.

I) 30SA/70LDH. Bar is 10 μm.

J) 20SA/80LDH. Bar is 10 μm.

K) 10SA/90LDH. Bar is 10 μm.

L) 0SA/100LDH. Bar is 10 μm.

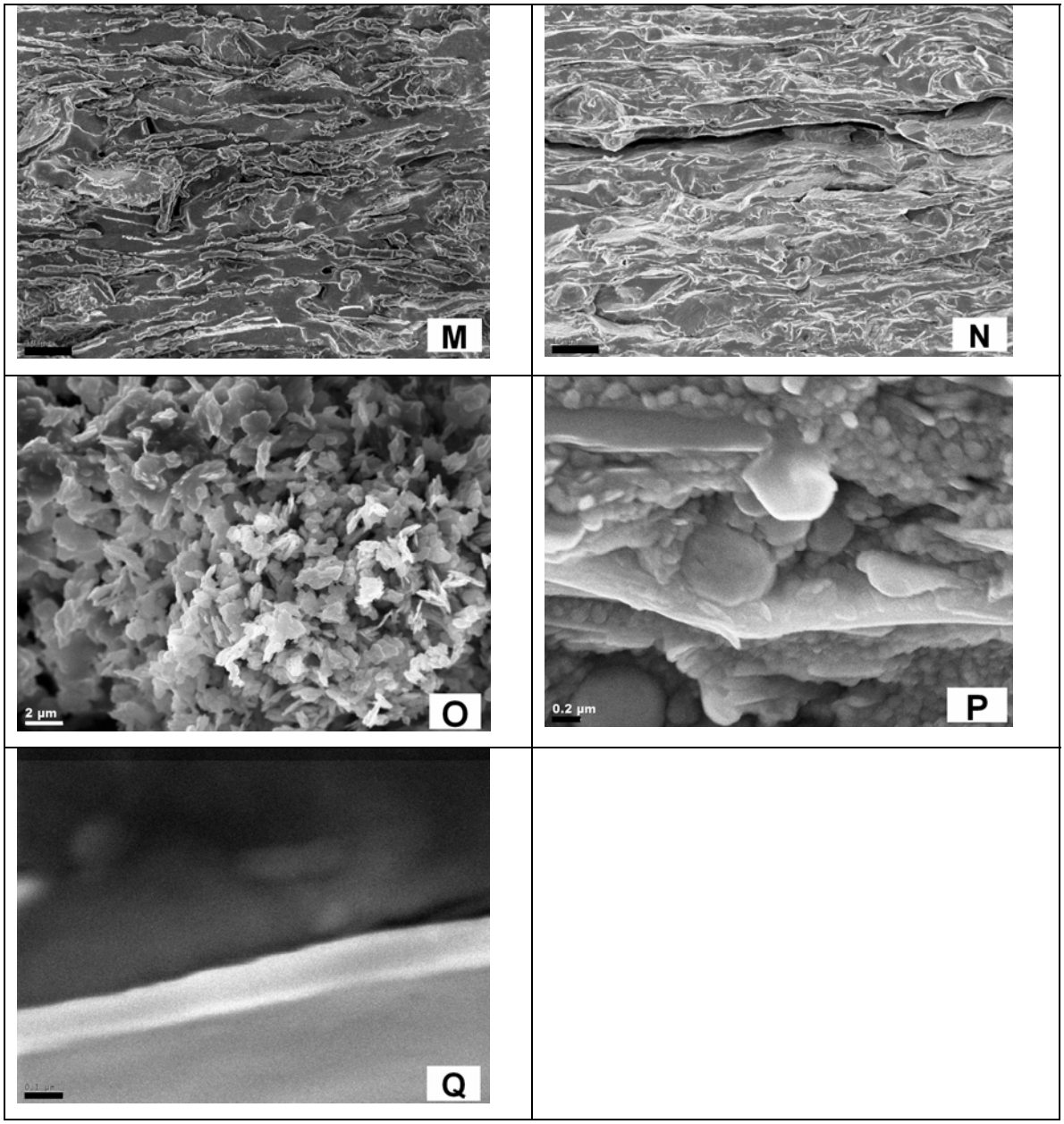

Figure 4-6 Scanning electron micrographs of the films.

M) 70SA/30bentonite. The bentonite is oriented within the film. Bar is 10 μm.

N) 70SA/30talc. The talc is oriented within the film. Bar is 10 μm.

O) Sand-rose structure of the LDH powder. Bar is 2 μm.

P) Large magnification of 80SA/20LDH showing intact LDH particle. Bar is 0,2 μm.

Q) Large magnification of 60SA/40LDH showing thickness of plates. Bar is 0,1 μm.

4.3.4. Optical Microscopy

When looking at film solutions which had a SA/LDH ratio of about 80/20 to 40/60, “needlelike” structures (Fig. 4-7) approximately 20 μm long could be seen. These “needles” are in actual fact plates of *ca*. 20 μm diameter (refer to SEM section) seen from the side. They are transparent from the top. This gives an explanation for why the film solutions are white, but form clear films upon drying. In the solution the large plate-like structures are oriented randomly, scattering the light passing through it, but upon drying, the plate-like structures are all oriented horizontally (as seen by SEM also).

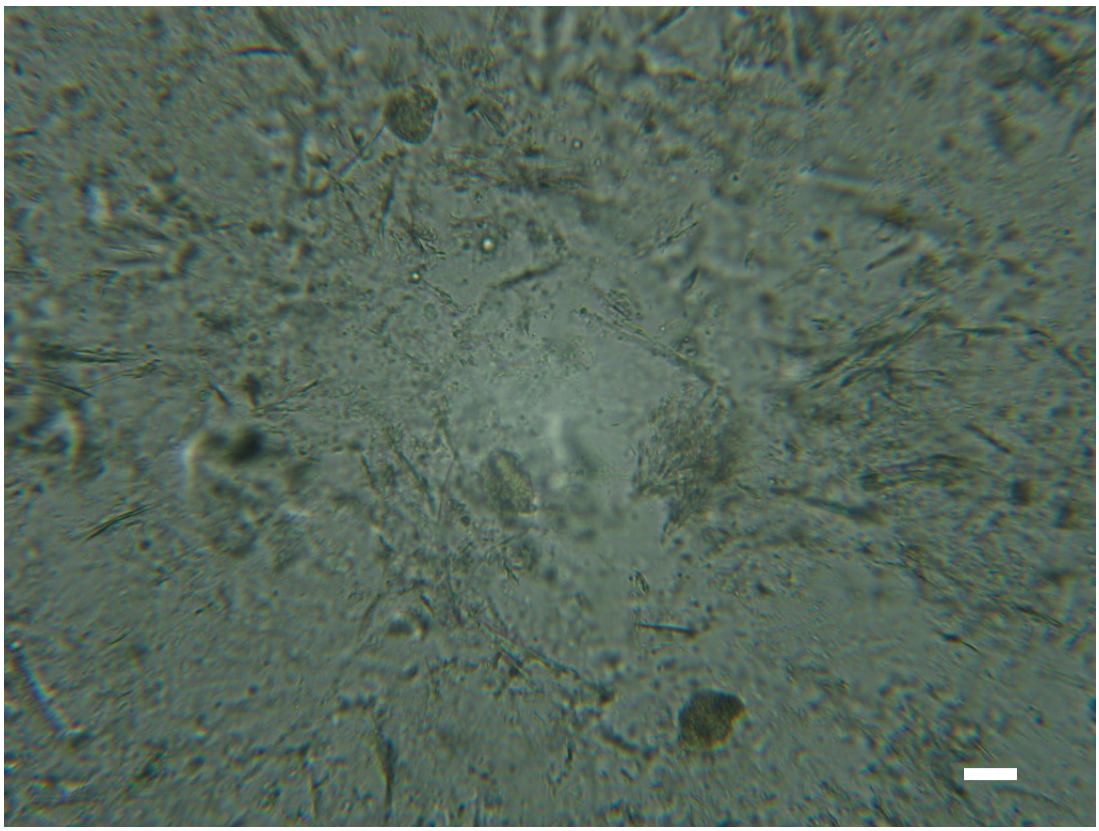

Figure 4-7 Optical microscope photo of the 60SA/40LDH film solution. Bar is 20 μm.

4.3.5. X-Ray Diffraction (XRD)

Depending on the amount of stearate present and the temperature employed, either a monolayer or bilayer could theoretically be intercalated (Fig. 4-8). The interlayer distance would be 32 Å for the monolayer and 52-53 Å for the bilayer. [10,17] Through molecular modelling calculations, Pospíšil *et al.* [18] reported a transition state between mono- and bilayer intercalation of octadecylammonium chloride in montmorillonite, with an interlayer distance of 47.8 Å.

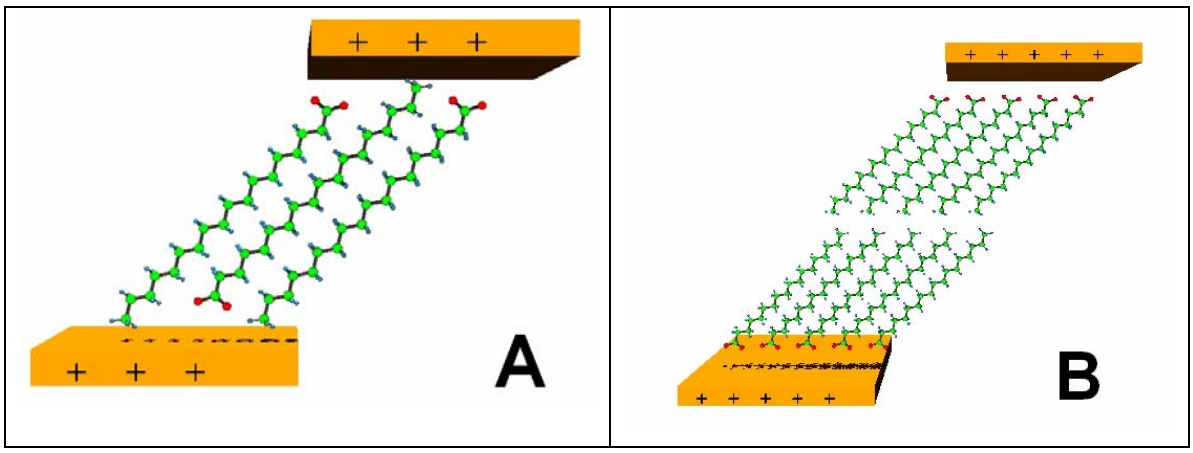

Figure 4-8 Monolayer (A) and bilayer (B) arrangement of stearate intercalated within LDH.

The XRD spectrum of the blank film (no LDH or SA) indicated a completely amorphous structure, with only a broad hump centred around 20° 2θ. The 100SA/0LDH film had a reflection at around 40 Å (due to the unreacted stearic acid bilayer, polymorph C [19]) and a small peak at about 8.1 Å due to the formation of some alginic acid (2-fold screw axis with fiber period of 8.7 Å, [20]). Upon the addition of LDH to the SA in the film, an interlayer distance of 52 Å is reached at the filler composition of 80SA/20LDH. With an increasing amount of LDH the intensity of the basal reflection and the interlayer distance decreased (Figs. 9 and 10), indicating that some exfoliation (delamination) took place at filler compositions in the region of 60SA/40LDH to 70SA/30LDH. The exfoliation behaviour around the middle of the series can be explained in terms of the exfoliation energy. Pospíšil *et al.* [18] calculated the exfoliation energy (total

interaction energy per supercell between two layers) of octadecylammonium chloride intercalated montmorillonite. It was found to decrease dramatically for the bilayer arrangements. In the 60SA/40LDH and 70SA/30LDH films, the interlayer distance should have been the largest (> 54 Å, lowest exfoliation energy), but due to exfoliation the higher interlayer distance reflections disappeared, and a lower interlayer distance phase remained, with a lower intensity. At the filler composition of 50SA/50LDH, the bilayer structure was present once again (basal reflection at 54 Å). Upon further increasing the LDH content (decreasing SA content), the basal spacing decreased again; this time not due to exfoliation but due to a lack of SA. Stearate intercalated to form structures between mono- and bilayers.

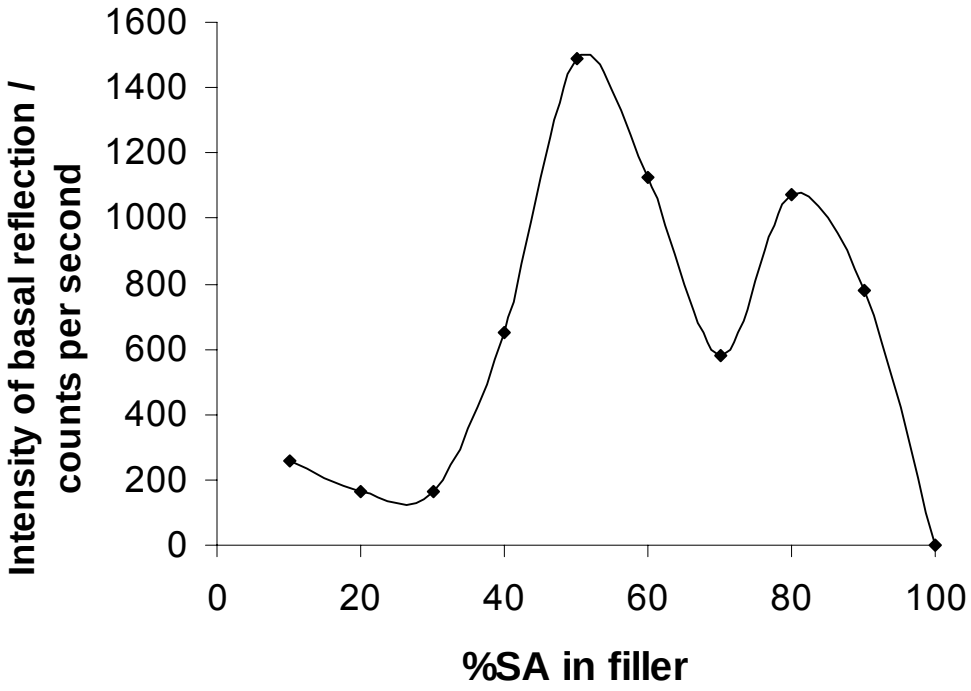

Figure 4-9 Variation in intensity of the basal reflection of the intercalated phase (LDH-SA) as function of filler composition. The dip in intensity indicated that exfoliation (delamination) took place.

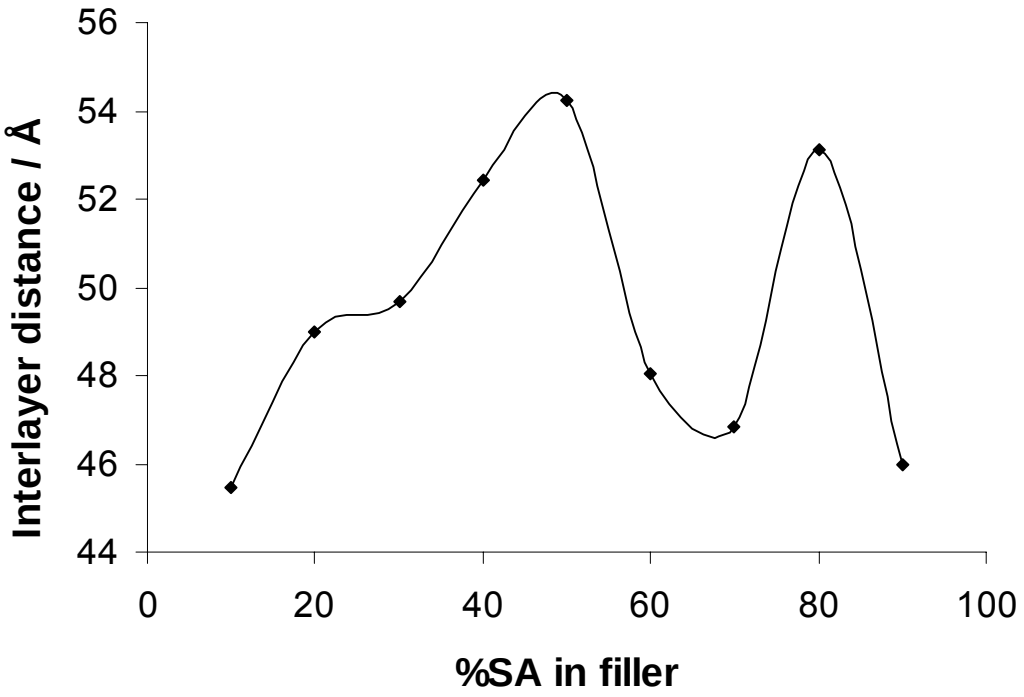

Figure 4-10 Variation of the interlayer distance of the intercalated phase (LDH-SA) as function of the filler composition. The dip in interlayer distance indicated that exfoliation took place, leaving only a phase with smaller interlayer distance.

Fig. 4-11 shows which crystalline phases were present in the 70SA/30LDH film at 10 minutes, 30 minutes and 60 minutes of reaction. At 10 minutes, almost no crystalline phases were present. The LDH basal reflection at 7.7 Å had a low intensity, because the LDH particles were still mostly agglomerated, settling to the bottom and not forming part of the cast film. At 30 minutes the sand-rose structures had broken down and the LDH particulates were suspended in the film solution. The 7.7 Å reflection was the most intense. Some LDH-SA had also formed at 30 minutes (52.2 Å). The 52.2 Å basal reflection had a higher intensity than the 17.9 Å (non-basal) reflection. At 60 minutes, however, the basal reflection reduced in intensity and interlayer distance (to 46.8 Å), with the 17.9 Å reflection being the most intense. This loss of intensity of the basal reflection is a strong indication that exfoliation took place between 30 and 60 minutes. It is

believed that the alginate, being a poly-anionic polysaccharide [21], aided the exfoliation of the LDH-SA without need for high shear mixing.

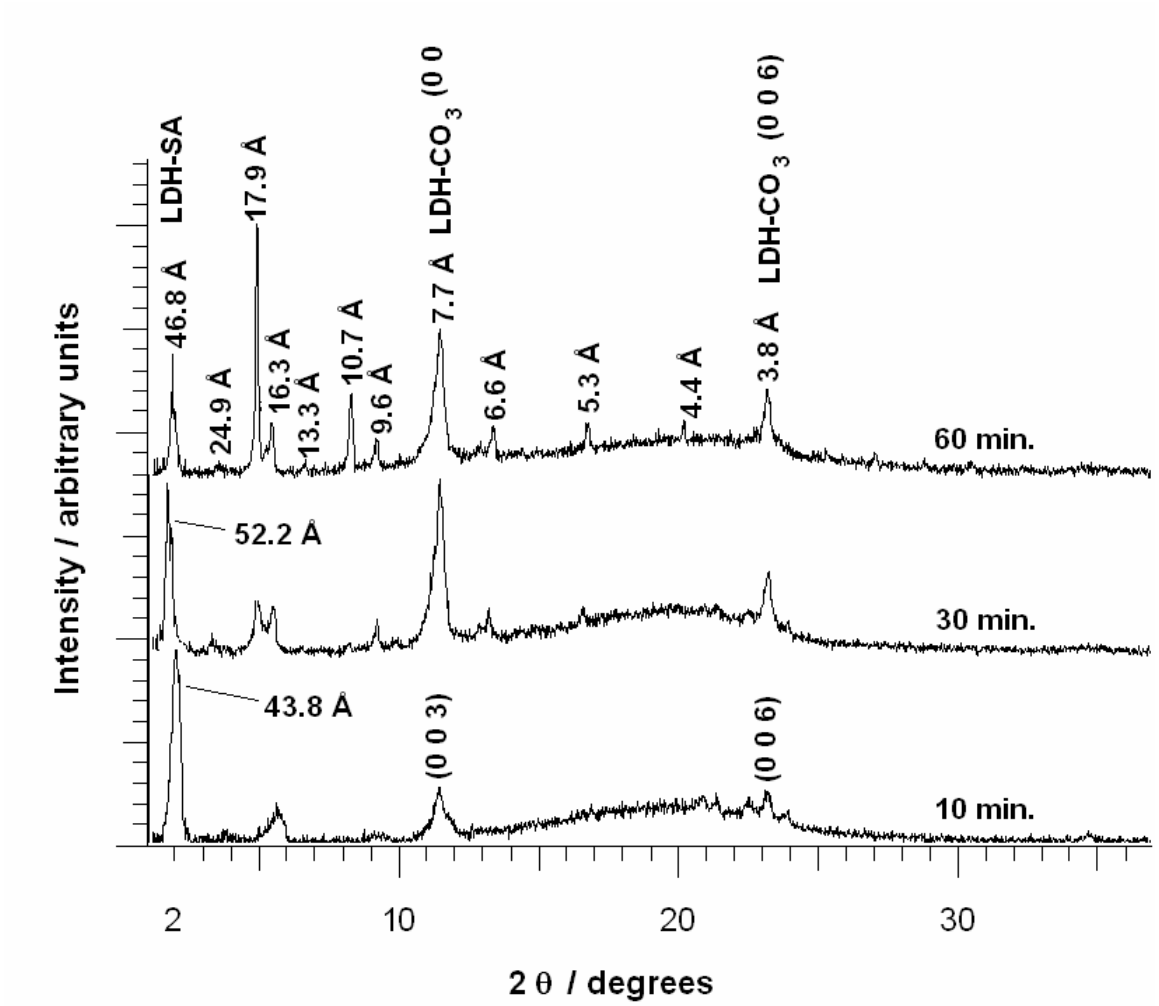

Figure 4-11 The crystalline phases present in the dried film 70SA/30LDH at 10, 30 and 60 minutes of reaction, showing the relative amounts of the LDH-CO_3 and LDH-SA phases and the lower interlayer distance LDH-SA phase remaining after exfoliation.

4.3.6. Tensile properties

Only the film 0SA/100 LDH has a higher tensile strength than the blank film. The other films (which all contain SA as well) are weaker due to the lack of mechanical strength of the SA (Fig. 4-12). All the films are less ductile (lower % strain at break) than the blank film except the film 70SA/30Talc (Fig. 4-13). It is unknown why the talc increased the ductility. The complete set of mechanical properties of these films can be seen in Appendix E.

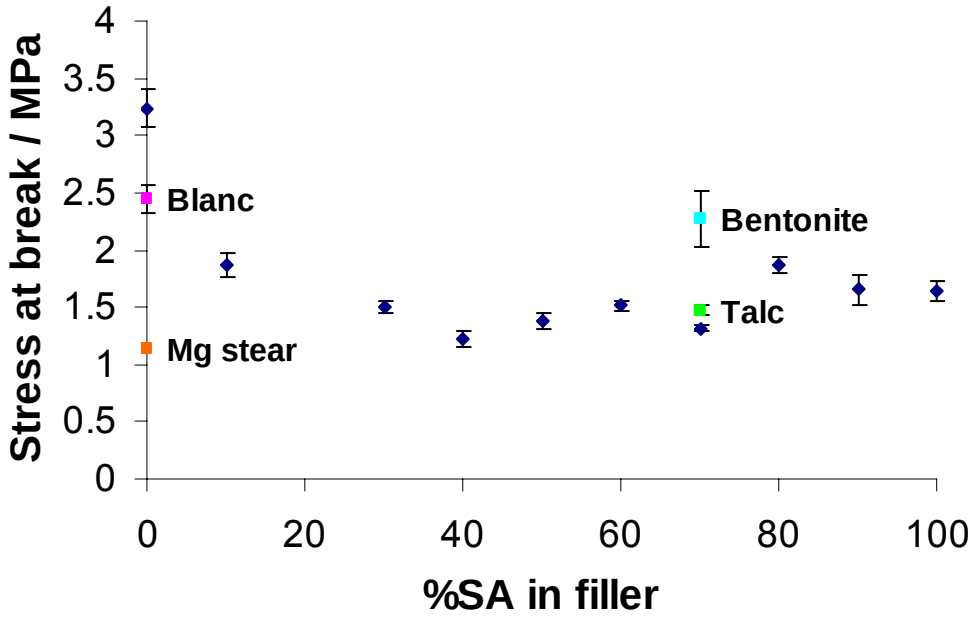

Figure 4-12 Stress at break of films as function of filler composition.

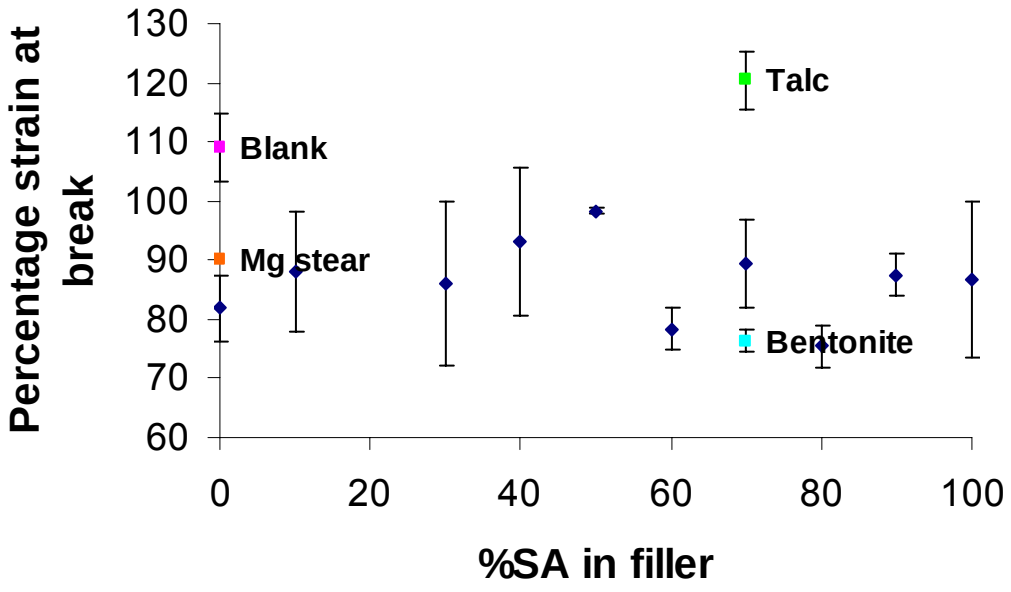

Figure 4-13 Percentage strain at break of films as function of filler composition.

The Young's moduli of our films were an order of magnitude lower and the elongation at break an order of magnitude larger than the starch films of Wilhelm *et al.* [6] because of the presence of the sodium alginate.

Fig. 4-14 shows the Young's moduli of films with different filler compositions. A maximum modulus was achieved at about 60SA/40LDH. This point probably corresponded to the minimum amount of SA needed to effectively break up the sand-rose structure in order to increase the surface area and efficiency of the reinforcing interaction between the LDH and the alginate, and possibly the dextrin. After the 60SA/40LDH point the amount of LDH available became less and thus also the reinforcing capabilities. The talc and bentonite, at the same mass %, did not have the same reinforcing effect (Fig. 4-14). For LDH we obtained a maximum increase in Young's modulus of 213% in comparison to the blank dextrin-alginate film. Wilhelm *et al*. [6] obtained only a 72% increase in modulus at 30% m/m loading of Ca^{2+} hectorite in comparison to pristine thermoplastic starch (glycerol-plasticized). De Carvalho *et al*. [5] observed a 50%

increase in modulus of starch/calcined kaolin composites at 50 phr kaolin (50 parts kaolin per 100 parts thermoplastic starch) in comparison to the pristine thermoplastic starch. Hence, the reinforcing capability of the LDH can probably be attributed to the electrostatic interaction between the positively charged LDH layers and the anionic alginate chains, which is absent in the case of talc and bentonite.

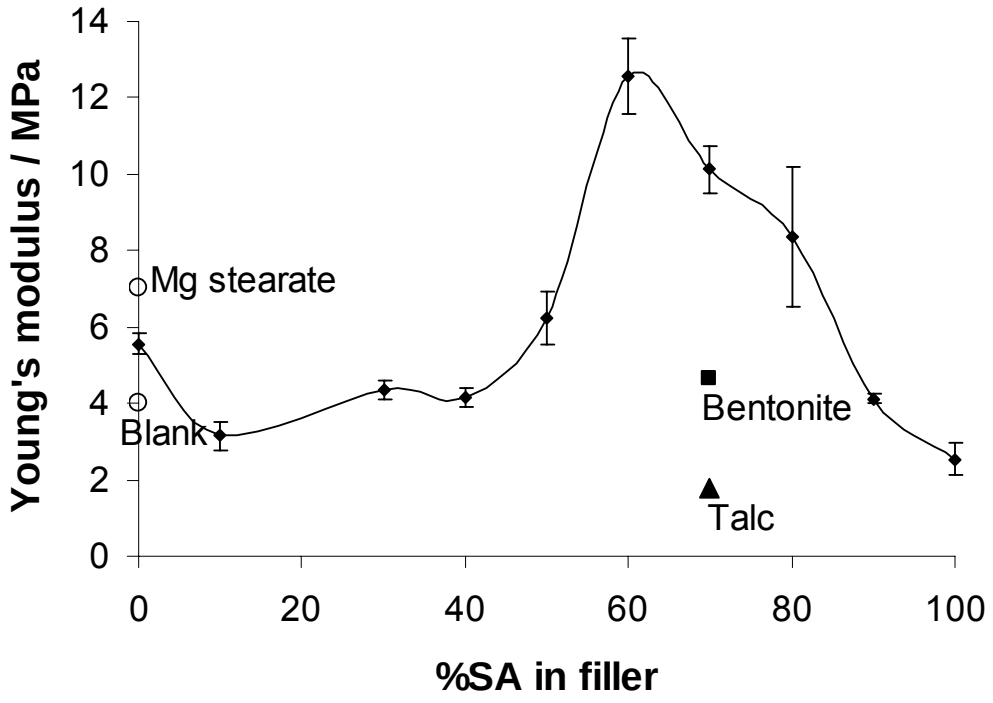

Figure 4-14 Young's moduli of films as function of filler composition.

Leaching of Mg^{2+} from the Mg_2Al-LDH used in this study (due to the presence of the acidic SA) was not expected because Hibino *et al*. [22] found that no leaching of Mg^{2+} cations took place in LDHs with Mg/Al ratio of 2 when treated with aqueous paramolybdate solutions (low pH), whereas substantial leaching took place in LDHs with Mg/Al ratios of 3 and 4. However, the presence of alginate might drive the leaching of some cations. When polymers with carboxylic acid groups (such as alginate) are neutralized with divalent or trivalent metal ions; the viscosity increases due to the formation of cross-links between polymer chains. [21,23,24] However, film solutions containing an equivalent amount of

magnesium stearate had a higher viscosity than LDH-SA containing films, indicating that more Mg^{2+} were available to cross-link the alginate and to increase Young's modulus (Fig. 4-14) [23].

4.3.7. XRD, tensile and WVP results revisited

The WVP, intensity of basal reflection and Young's modulus data show correlated trends (Fig. 4-15). The curve of the intensity of the basal reflection of the LDH-SA and the curve of Young's moduli crossed midway between 50% and 60% SA. Below the 60% SA point in these curves, the intensity of the basal reflection was high, indicating that no exfoliation took place; consequently the modulus dropped drastically. The opposite is true between 60 and 70% SA (the moduli were high and the intensity of the basal reflections were low, indicating exfoliation). Hence, the hypothesis that exfoliation (or delamination) of the LDH-SA caused the increase in Young's modulus was further supported.

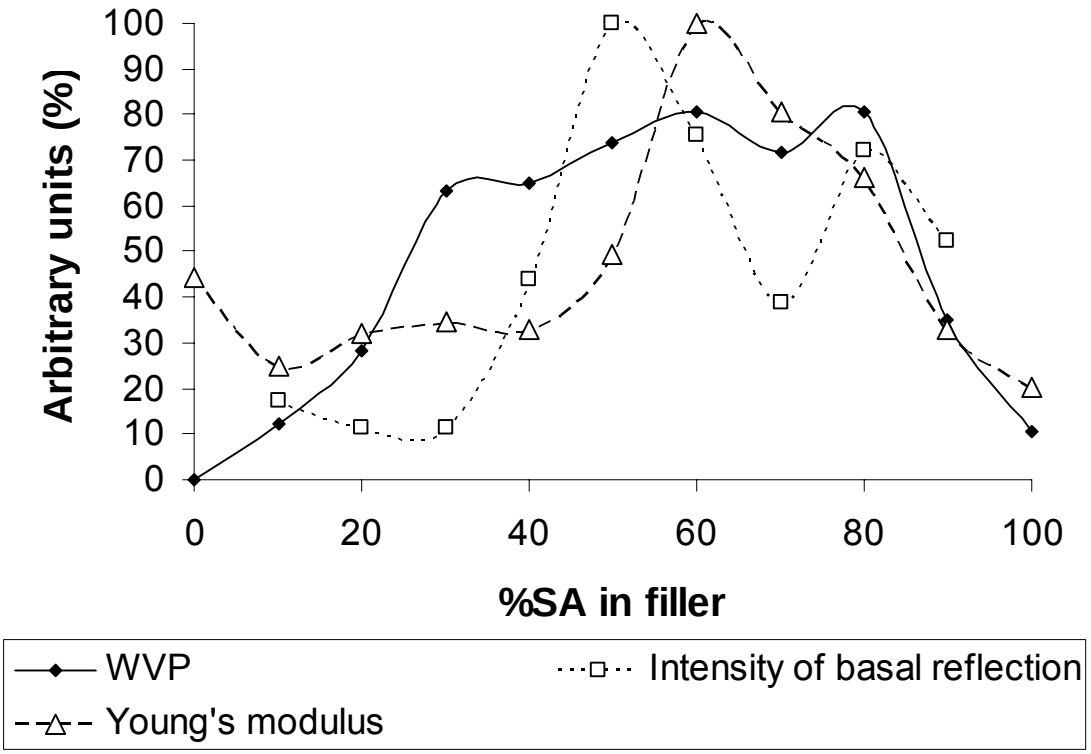

Figure 4-15 Comparison of WVP, Young's modulus and intensity (XRD) data as function of filler composition. WVP values of Fig. 4-4 were subtracted from 100 for this graph.

4.4. Conclusions

The combination of SA and LDH improves the WVP with respect to the use of only SA or only LDH. We believe that the use of the combination of a fatty acid (rather than any other acid) and a LDH is the most beneficial for preparation of films with low WVP because the fatty acid in itself lowers the WVP, it can intercalate into the LDH to form the large plate-like barriers and *in situ* leaching of LDH cations with concomitant cross-linking of the alginate can occur. Also, exfoliation of the LDH-SA by the poly-anionic alginate was evidenced. More research needs to be done in order to determine the contributions of the two mechanisms (exfoliation vs. cross-linking) to the increased Young's modulus (increased stiffness) and decreased WVP, but from qualitative viscosity

observations it seems that cross-linking due to leaching of Mg^{2+} from the LDH plays only a minor role.

References

1 Y. WU, C.L. WELLER, F. HAMOUZ, S. CUPPETT and M. SCHNEPF, *J. Food Sci.* **66** (2001) 486.

2 O.R. FENNEMA, S.L. KAMPER and J.J. KESTER, USP 4 915 971, Method for making an edible film and for retarding water transfer among multi-component food products, 10 April 1990.

3 R.J. AVENA-BUSTILLOS and J.M. KROCHTA, *J. Food Sci*. **58** (1993) 904.

4 M. ALEXANDRE and P. DUBOIS, *Mater. Sci. and Eng. R* **28** (2000) 1.

5 A.J.F. DE CARVALHO, A.A.S. CURVELO and J.A.M. AGNELLI, *Carbohydr. Polym.* **45** (2001) 189.

6 H.-M. WILHELM, M.-R. SIERAKOWSKI, G.P. SOUZA and F. WYPYCH, *Carbohydr. Polym.* **52** (2003) 101.

7 H.-M. WILHELM, M.-R. SIERAKOWSKI, G.P. SOUZA and F. WYPYCH, *Polym. Int.* **52** (2003) 1035.

8 D.W.S. WONG, K.S. GREGORSKI, J.S. HUDSON and A.E. PAVLATH, *J. Food Sci.* **61** (1996) 337.

9 S. MIYATA and T. KUMURA, *Chem. Lett.* (1973) 843.

10 T. ITOH, N. OHTA, T. SHICHI, T. YUI and K. TAKAGI, *Langmuir* **19** (2003) 9120.

11 M. ADACHI-PAGANO, C. FORANO and J.-P. BESSE, *Chem. Commun.* (2000) 91.

12 A. WEXLER, in “Handbook of Physics and Chemistry”, 79th edition, edited by D.R. Lide (CRC Press, Boca Raton, 1998) p. ***15***-25.

13 J.M. KROCHTA and C. DE MULDER-JOHNSTON, *Food Technol.* **51** (1997) 61.

14 M. BORJA and P.K. DUTTA, *J. Phys. Chem.* **96** (1992) 5434.

15 T. HABIG McHUGH, R. AVENA-BUSTILLOS and J.M. KROCHTA, *J. Food Sci.* **58** (1993) 899.

16 J.X. HE, S. YAMASHITA, W. JONES and A. YAMAGISHI, *Langmuir* **18** (2002) 1580.

17 T. KANOH, T. SHICHI and K. TAKAGI, *Chem. Lett.* (1999) 117.

18 M. POSPÍŠIL, P. ČAPKOVÁ, Z. WEISS, Z. MALÁČ and J. ŠIMONÍK, *J. Colloid Interface Sci.* **245** (2002) 126.

19 J.F. MEAD, R.B. ALFIN-SLATER, D.R. HOWTON and G. POPJÁK, in "Lipids: Chemistry, Biochemistry and Nutrition" (Plenum Press, New York, 1986) p. 53.

20 W.T. ASTBURY, *Nature* **155** (1945) 167.

21 R.L. WHISTLER and J.N. BeMILLER, in "Carbohydrate Chemistry for Food Scientists" (Eagan Press, St. Paul, Minnesota, 1997) p. 196.

22 T. HIBINO and A. TSUNASHIMA, *Chem. Mater.* **9** (1997) 2082.

23 M. FUJIYAMA, K. YAMANE, K. AYAMA and H. INATA, *J. Appl. Polym. Sci.* **86** (2002) 2887.

24 F. YOKOYAMA, E.C. ACHIFE, M. MATSUOKA, K. SHIMAMURA, Y. YAMASHITA and K. MONOBE, *Polymer* **32** (1991) 2911.